

Measurement of Low-temperature Loss Tangent of High-resistivity Silicon Wafers with High Q-factor Superconducting Resonators

M. Checchin,* D. Frolov, A. Lunin, A. Grassellino, and A. Romanenko

*Superconducting Quantum Materials and Systems Center,
Fermi National Accelerator Laboratory, Batavia IL 60510, USA*

(Dated: November 9, 2021)

In this letter, we present the first direct loss tangent measurement of high-resistivity (100) silicon wafers in the temperature range from ~ 70 mK to 1 K, approaching the quantum regime. The measurement was performed using an innovative technique that utilizes a high quality factor superconducting niobium resonator and allows to directly measure the loss tangent of insulating materials with an unprecedented level of accuracy and precision. We report silicon loss tangent values at the lowest temperature and for electric field amplitudes comparable to those found in planar transmon devices one order of magnitude larger than what was previously assumed. In addition, we discover a non-monotonic trend of the loss tangent as a function of temperature that likely indicates the existence of unexplored microwave dissipation mechanisms in high-resistivity silicon at milli-Kelvin temperatures. This seminal study lays the foundations for a novel approach to uncover and understand unexplored loss mechanisms in insulating materials in the quantum regime, aiming to maximize coherence in quantum devices.

Superconducting quantum circuits based on cavity-quantum electrodynamics architecture [1–3] represent a leading technology for constructing quantum processors and achieving quantum supremacy [4]. This technology utilizes the nano-fabrication processes developed by the semiconductor industry to manufacture integrated microwave circuits. Silicon is a vital material in integrated circuit technology; therefore, it is the substrate of choice for superconducting quantum bit fabrication.

Because of the high dielectric constant ($\epsilon_r' = 11.5$ at low temperatures), a large fraction of the electromagnetic energy is stored in the silicon substrate [5]; hence, its contribution to the overall device energy loss can be substantial. Accurate knowledge of the Si loss tangent is thus pivotal for correctly estimating dissipation in quantum devices.

High-resistivity silicon (Si) ($\rho \geq 5$ k Ω -cm) at milli-Kelvin temperatures and microwave frequencies is generally assumed to introduce negligible dielectric losses compared to the native oxide and substrate-metallization intermixing layers found in typical superconducting quantum devices. However, no direct measurements of Si wafer loss tangent at milli-Kelvin temperatures have been presented thus far. Therefore, a reasonable large degree of uncertainty on the actual Si loss tangent value in the milli-Kelvin range still exists. Loss tangent data of Si at milli-Kelvin temperatures exist for silicon billets [6], which are not a representative sample of the wafers used to fabricate quantum bits, and for high-resistivity silicon at higher temperatures [7].

In this letter, we present the first direct measurement of the loss tangent of high-resistivity floating zone (FZ) silicon wafers in the temperature range from ~ 70 mK to 1 K. We discover a non-monotonic trend of the loss tangent of silicon with temperature qualitatively explained by a combination of conduction-type losses and

an unidentified loss channel. Additionally, we demonstrate that the milli-Kelvin Si loss tangent is one order of magnitude larger than expected [5, 8, 9].

Measurements were performed using a high quality factor (Q-factor) elliptical superconducting niobium resonator hosting the Si sample in the high electric field region. The fundamental mode TM_{010} resonating at 2.6 GHz was used to perform the sample characterization over the entire temperature range.

Elliptical superconducting resonators are typically adopted in particle accelerators at liquid He temperatures to accelerate relativistic charged particles because of their high efficiency (intrinsic Q-factor $Q_0 \sim 10^{11}$) in producing accelerating gradients on the order of tens of MV/m [10]. Nonetheless, they also allow for $Q_0 \gtrsim 10^9$ at 10 mK [11], making them an ideal tool for performing loss tangent measurements of insulators with a high degree of accuracy at milli-Kelvin temperatures.

Fig. 1 (a) shows a 3D model of the experimental setup. The resonator was secured to the mixing chamber plate of a dilution refrigerator (DR). The input line had several stages of attenuation for a total of ~ 60 dB, including the Eccosorb filters. The output line had isolators and Eccosorb filters connected immediately after the device output port and a 35 dB low-noise HEMT amplifier, which was thermalized to the quasi-4 K plate (typically stable at approximately 2.4 K). A simplified scheme of microwave connections in the DR is shown in Fig. 1 (b). The total gain of the transmitted line was measured to be approximately 62 dB, including a warm 40 dB amplifier (not shown in the schematics of Fig. 1 (b)).

Intrinsic FZ Si(100) single-side polished wafers, with a thickness of 675 μm , were procured with room temperature resistivity of 10 k Ω -cm and diced to 10 cm long and 2 mm wide strips. After dicing, one sample was cleaned in an ultrasonic bath of isopropyl alcohol for 15 min, dried

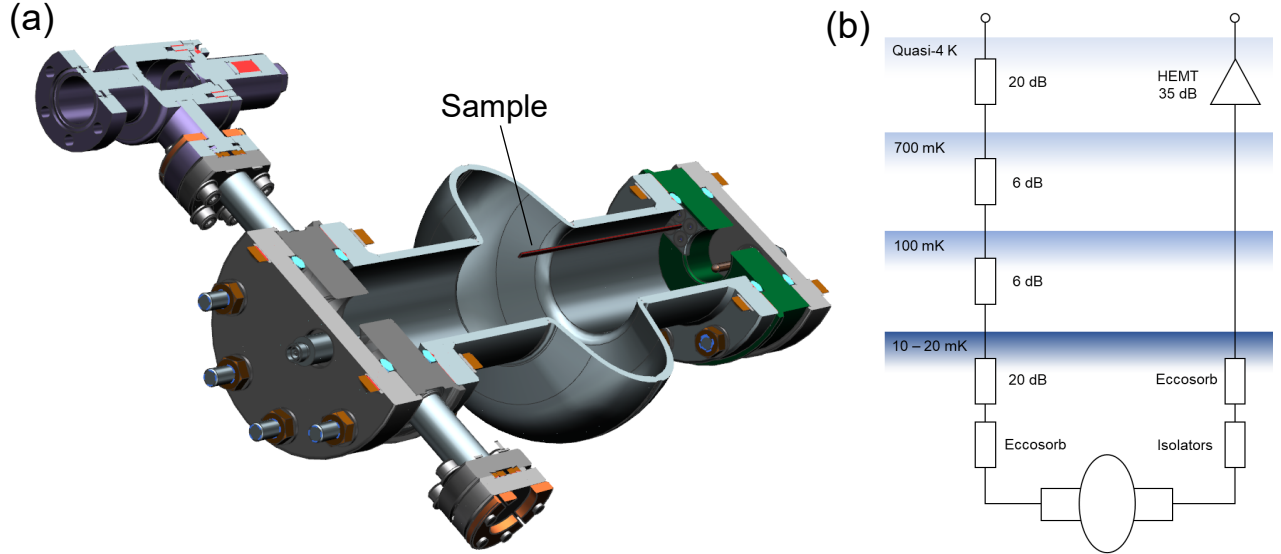


FIG. 1. Experimental set-up. (a) Three dimensional (3D) model of the experimental setup with the sample highlighted. (b) Schematic of the experiment in the dilution refrigerator.

in ultra-pure nitrogen, assembled to the resonator, and subsequently pumped to a vacuum level of $p < 10^{-5}$ Torr.

The loaded Q-factor (Q_L) was measured in decay mode. A steady-state electromagnetic field was established in the resonator and the transmitted power (P_t) free decay was recorded as a function of time after shutting off the power fed to the device. The maximum electric field on the Si sample is measured to be approximately 10 V/m, corresponding to an average number of photons stored in the resonator in the order of $\langle n \rangle \sim 10^{10}$. To be notice that independently on the number of photons reached in the resonator, the actual electric field values experienced by the Si sample in this experiment are of the same order of magnitude of those found in typical transmon devices in the near surface of the substrate [12].

We define Q_L as $Q_L = -10\omega/\ln 10(dP_t/dt)^{-1}$, where ω denotes the angular frequency, and dP_t/dt is the angular coefficient of the transmitted power free decay—with power measured in dBm. This strategy to measure Q_L was implemented to increase the measurement accuracy and circumvent the typical S21 measurement approach that is limited by distortions of the resonant peak and appearance of side bands generated by microphonics [13] as a consequence of the high Q_L . Additional details regarding this measurement strategy are reported in Ref. [11 and 14].

In Fig. 2, we illustrate the loaded Q-factor measured as a function of temperature. Blue dots and navy triangles represent the loaded Q-factor (Q_L) data acquired in this study and plotted against the temperature of the sample—measured at the flange where the sample is attached—and of the mixing chamber, respectively. The light blue diamonds show the intrinsic Q-factor of the

resonator alone, without the Si sample, as measured in Ref. [11]. The temperature variance between the blue dots and navy triangles is caused by the not ideal thermal path connecting the sample to the mixing chamber. At thermal equilibrium, the sample could not be cooled below 73 mK.

The loss tangent of the sample is calculated as follows:

$$\frac{1}{Q_S} = \frac{p_{Si}}{Q_{Si}} + \frac{p_{SiO_2}}{Q_{SiO_2}} = \frac{1}{Q_L} - \frac{1}{Q_0} - \frac{1}{Q_1} - \frac{1}{Q_2}, \quad (1)$$

where $Q_1 = 5.8 \cdot 10^9$ and $Q_2 = 5 \cdot 10^{14}$ represent the external Q-factors of the antennas measured for the same setup in a liquid helium bath at 1.5 K, as described in Ref. [15], whereas $p_{Si} = 9 \cdot 10^{-4}$ and $p_{SiO_2} = 3 \cdot 10^{-9}$ denote the participation ratios of silicon and the native silicon oxide layer, defined as follows: $p_{diel} = \int_{V_{diel}} \varepsilon_{diel} |\mathbf{E}|^2 dV_{diel} / \int_V \varepsilon_0 |\mathbf{E}|^2 dV$. Both values were calculated using finite-element simulations by the high-frequency structure simulator (HFSS) program.

It is important to highlight that the measured loaded Q-factor is dominated by the sample loss, whereas the other contributions are negligible. In fact, Q_0 is approximately one order of magnitude higher than Q_L at the lowest temperature, whereas for temperature levels approaching 1 K, it is two orders of magnitude higher (see Fig. 2), and both Q_1 and Q_2 are at least one order of magnitude higher than Q_L . This implies that the measurement strategy implemented is very accurate and is not affected by dissipation mechanisms extrinsic to the sample under study.

The loss tangent of SiO_2 at milli-Kelvin temperatures is experimentally known to be approximately $1/Q_{SiO_2} \simeq 5 \cdot 10^{-3}$ [16]. For the geometry under study, the par-

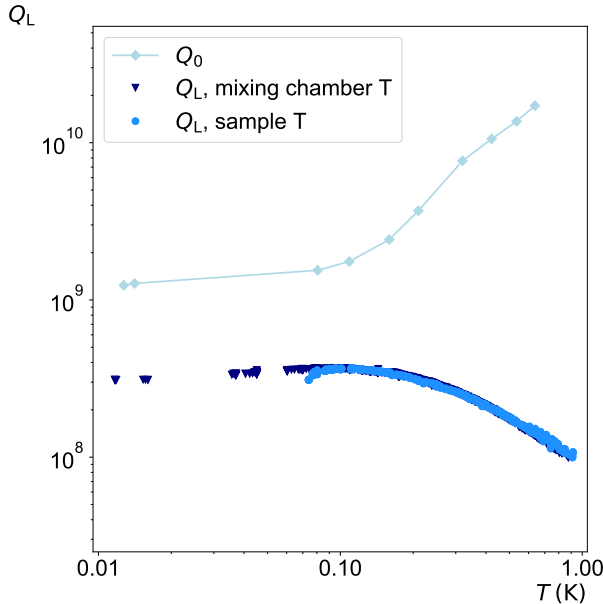


FIG. 2. Loaded quality factor as a function of temperature. Navy points plotted as a function of the mixing chamber temperature and blue points plotted as a function of sample temperature. The resonator intrinsic Q-factor versus temperature at 2.6 GHz was reported in Ref. [11] and it is shown in light blue.

ticipation ratio of the SiO_2 layer is calculated to be $p_{\text{SiO}_2} = 3 \cdot 10^{-9}$. Therefore, SiO_2 contribution to Q_L is $Q_{\text{SiO}_2}/p_{\text{SiO}_2} \sim 10^{11}$, hence negligible compared to that of silicon. We can then define the silicon loss tangent as follows:

$$\frac{1}{Q_{\text{Si}}} = \frac{1}{p_{\text{Si}} Q_S}. \quad (2)$$

Fig. 3 shows the loss tangent of silicon measured as a function of temperature. Similar to the previous graph, the navy triangles represent the data plotted against the mixing chamber temperature, whereas the blue points represent the data plotted against the sample temperature.

At the lowest temperature, 73 mK, the loss tangent is equal to $2.7 \cdot 10^{-6}$, which is in agreement with measurements performed on silicon billets in whispering gallery mode configuration [6]. In contrast, our experiment recorded higher values compared to indirect estimations based on measurements and simulations of planar devices [5, 8, 9], which are in the order of 10^{-7} , one order of magnitude lower than our experimental observations.

We observe a non-monotonic dependence of the silicon loss tangent on temperature, which does not resemble the two-level system (TLS) temperature dependence. The value of $1/Q_{\text{Si}}$ decreases with decreasing temperature, reaching a minimum at approximately 100 mK. Below 100 mK, the trend is opposite, and the loss tangent

increases as the temperature decreases with a steeper slope. This trend is better appreciated in the inset of Fig. 3, where the temperature is shown on a linear scale. The shaded areas show the experimental errors associated with the measurement. This was calculated through error propagation, where the error in Q_L was propagated from the square root of the variance of the angular coefficient that was calculated by the linear regression routine; the errors in Q_0 , Q_1 , and Q_2 were assumed to be 10% while that in p_{Si} was estimated to be 25%, and it was calculated through HFSS simulations assuming ± 2 mm sample misalignment and $11.5 \leq \varepsilon'_r \leq 11.9$.

In addition to TLS dissipation, conduction losses in semiconducting materials might also contribute to the loss tangent. Consequently, the dielectric constant is expressed as follows:

$$\varepsilon = \varepsilon'_r - i \left(\varepsilon''_r + \frac{\sigma}{\omega \varepsilon_0} \right), \quad (3)$$

where ε'_r and ε''_r represent the real and imaginary parts of the complex dielectric constant, whereas σ denotes the low temperature conductivity. The loss tangent is thereafter expressed as follows:

$$\frac{1}{Q_{\text{Si}}} = \frac{1}{Q_{\text{diel}}} + \frac{\sigma}{\omega \varepsilon_0 \varepsilon'_r}, \quad (4)$$

where the first term $1/Q_{\text{diel}} = \varepsilon''_r / \varepsilon'_r$ denotes the dielectric loss tangent dominated by dielectric dissipation

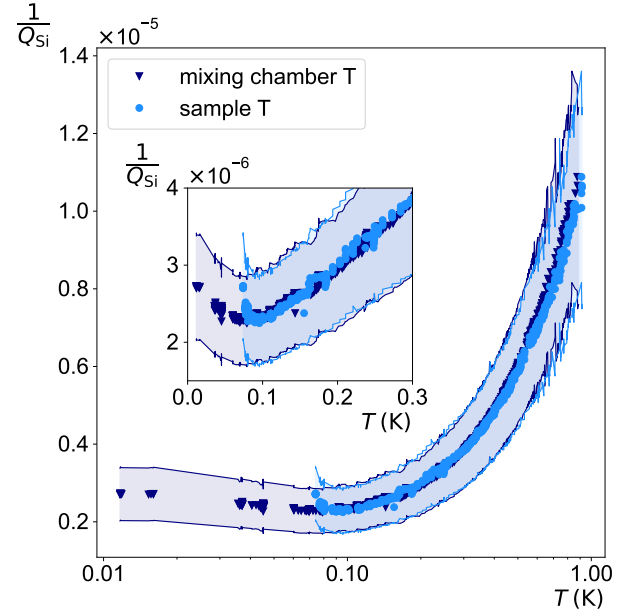


FIG. 3. Silicon loss tangent as a function of temperature. Blue points plotted as a function of the mixing chamber temperature and light blue points plotted as a function of sample temperature. The inset is a zoom of the data with temperature on a linear scale.

(TLS), whereas the second term represents the conduction loss tangent dominated by conduction losses.

We identify the increasing trend of the loss tangent with temperature above ~ 100 mK with the second term of Eq. 4, and particularly with the occurrence of an electron hopping mechanism, likely variable range hopping [17]. Variable range hopping conduction may take place at low temperatures where localized states close to the Fermi level within $\sim \kappa_B T$ can contribute to the overall conduction; conduction becomes dominated by hops between levels that are closer in energy, even if spatially far apart and with small wave function overlap. Because of variable range hopping, the loss tangent decreases with $\sim \exp(-T^{-1/4})$, and for $T \rightarrow 0$, it should exponentially approach zero [17]. In contrast, we observed that for $T < 100$ mK, the loss tangent inverts the slope and increases as temperature is lowered.

Although TLS dissipation might qualitatively describe the low-temperature trend as $1/Q_{\text{diel}}$ increases with decreasing temperatures with $\sim \tanh(1/T)$ [18], its nature is unknown. Alternatively, non-linearity in the hopping conductivity for a finite electric field amplitude at very low temperatures could also qualitatively explain the low-temperature trend [19, 20]. In any case, no conclusive statement on the origin of the low-temperature trend can be drawn at the current stage, and more experiments are needed.

In conclusion, we described a novel and accurate method to directly measure the loss tangent of insulating materials in wafer form using high Q-factor superconducting resonators. We reported the first direct measurement of the loss tangent of a high-resistivity silicon wafer in the temperature range from ~ 70 mK to 1 K. Furthermore, we showed that the loss tangent of high-resistivity Si in the milli-Kelvin range is one order of magnitude higher than that previously indirectly estimated from measurements and simulations of planar devices [5, 8, 9], although it is in agreement with values obtained from whispering gallery measurements of Si billets [6]. In addition, we discover a non-monotonic behavior of the loss tangent dependence on temperature with a minimum at approximately 100 mK, which is currently under investigation.

The methodology developed in this study will serve as a tool for detailed investigation of losses in dielectrics at milli-Kelvin temperatures, and guide the selection of materials for the fabrication of high-coherence quantum devices.

This material is based on work supported by the U.S. Department of Energy, Office of Science, National Quantum Information Science Research Centers, Supercon-

ducting Quantum Materials and Systems Center (SQMS) under contract number DE-AC02-07CH11359.

* checchin@fnal.gov

- [1] A. Wallraf, D. I. Schuster, A. Blais, L. Frunzio, R.-S. Huang, J. Majer, S. Kumar, S. M. Girvin, and R. J. Schoelkopf, *Nature* **431**, 162 (2004).
- [2] R. J. Schoelkopf and S. M. Girvin, *Nature* **451**, 664 (2008).
- [3] M. H. Devoret and R. J. Schoelkopf, *Science* **339**, 1169 (2013).
- [4] F. Arute and et al., *Nature* **574**, 505 (2019).
- [5] C. Wang, C. Axline, Y. Y. Gao, T. Brecht, Y. Chu, L. Frunzio, M. H. Devoret, and R. J. Schoelkopf, *Appl. Phys. Lett.* **107**, 162601 (2015).
- [6] J. Bourhill, M. Goryachev, D. L. Creedon, B. C. Johnson, D. N. Jamieson, and M. E. Tobar, *Phys. Rev. Applied* **11**, 044044 (2019).
- [7] J. Krupka, J. Breeze, A. Centeno, N. Alford, T. Claussen, and L. Jensen, *IEEE Trans. Microw. Theory Tech.* **54**, 3995 (2006).
- [8] W. Woods, G. Calusine, A. Melville, A. Sevi, E. Golden, D. K. Kim, D. Rosenberg, J. L. Yoder, and W. D. Oliver, *Phys. Rev. Applied* **12**, 014012 (2019).
- [9] A. Melville, G. Calusine, W. Woods, K. Serniak, E. Golden, B. M. Niedzielski, D. K. Kim, A. Sevi, J. L. Yoder, E. A. Dauler, and W. D. Oliver, *Appl. Phys. Lett.* **117**, 124004 (2020).
- [10] A. Romanenko, A. Grassellino, A. C. Crawford, D. A. Sergatskov, and O. Melnychuk, *Appl. Phys. Lett.* **105**, 234103 (2014).
- [11] A. Romanenko, R. Pilipenko, S. Zorzetti, D. Frolov, M. Awida, S. Belomestnykh, S. Posen, and A. Grassellino, *Phys. Rev. Applied* **13**, 034032 (2020).
- [12] J. Lisenfeld, A. Bilmes, A. Megrant, R. Barends, J. Kelly, P. Klimov, G. Weiss, J. M. Martinis, and A. V. Ustinov, *Npj Quantum Inf.* **5**, 105 (2019).
- [13] H. Padamsee, J. Knobloch, and T. Hays, *RF Superconductivity for Accelerators* (Wiley-VCH Verlag GmbH and Co., KGaA, Weinheim, 2008).
- [14] A. Romanenko and D. I. Schuster, *Phys. Rev. Lett.* **119**, 264801 (2017).
- [15] O. Melnychuk, A. Grassellino, and A. Romanenko, *Rev. Sci. Instrum.* **85**, 124705 (2014).
- [16] J. M. Martinis, K. B. Cooper, R. McDermott, M. Steffen, M. Ansmann, K. D. Osborn, K. Cicak, S. Oh, D. P. Pappas, R. W. Simmonds, and C. C. Yu, *Phys. Rev. Lett.* **95**, 210503 (2005).
- [17] N. F. Mott, *J. Non-Cryst. Solids* **1**, 1 (1968).
- [18] C. Müller, J. H. Cole, and J. Lisenfeld, *Rep. Prog. Phys.* **82**, 124501 (2019).
- [19] N. Apsley and H. P. Hughes, *Philos. Mag.* **30**, 963 (1974).
- [20] N. Apsley and H. P. Hughes, *Philos. Mag.* **31**, 1327 (1975).